# Optical Spectroscopy of Graphene Quantum Dots: The Case of C132

**ARTICLE** *in* THE JOURNAL OF PHYSICAL CHEMISTRY A · JUNE 2014

Impact Factor: 2.69 · DOI: 10.1021/jp502753a · Source: PubMed



**3 AUTHORS**, INCLUDING:

Christian Wiebeler
Universität Paderborn
**14** PUBLICATIONS **47** CITATIONS
SEE PROFILE

Stefan Schumacher
Universität Paderborn
**75** PUBLICATIONS **497** CITATIONS
SEE PROFILE

THE JOURNAL OF PHYSICAL CHEMISTRY A

Article

pubs.acs.org/JPCA

# Optical Spectroscopy of Graphene Quantum Dots: The Case of C132

Hans Riesen,*[,†] Christian Wiebeler,[‡] and Stefan Schumacher[‡]

[†]School of Physical, Environmental and Mathematical Sciences, The University of New South Wales, Canberra, Australian Capital Territory 2600, Australia

[‡]Department of Physics and Center for Optoelectronics and Photonics Paderborn (CeOPP), University of Paderborn, Warburger Straße 100, 33098 Paderborn, Germany

Supporting Information

**ABSTRACT:** We have reinvestigated the optical spectroscopy of C132 graphene quantum dots by absorption, selective fluorescence, excitation and time-resolved spectroscopy, the external heavy atom effect, and DFT based quantum chemical calculations. In particular, wavelength-selective photobleaching provides strong evidence for the assignment of the intrinsic absorption and emission features of the quantum dots and indicates that emissions observed at ~670 and ~630 nm and associated relatively narrow features that display vibrational progressions in the selective excitation spectra are due to different species. The emitting state that leads to a broad emission (1700 $cm^{-1}$) centered around 750 nm appears to be a "near-dark" singlet state with a relatively long lifetime of ~30 ns. Simulated spectra, based on the nuclear ensemble approach, are in qualitative agreement with this finding and indicate very low oscillator strengths with some significant electron-vibrational intensity borrowing.

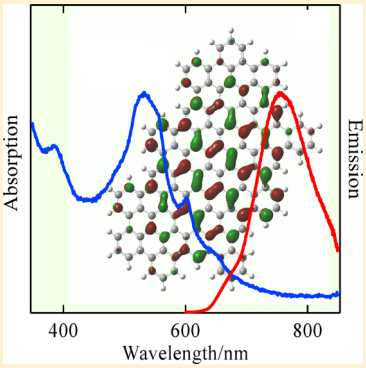


## 1. INTRODUCTION

With the discovery of C60, carbon nanotubes, and most recently graphene, carbonaceous materials have received a great deal of interest over the past 3 decades.[1−4] Also, nanodiamonds have been the subject of numerous investigations,[5] and this has been largely driven by their unique properties for applications as optical and magnetic probes.[6]

Over recent years, in particular graphene, consisting of two-dimensional (2D) single-atom carbon sheets, has been at the center of numerous investigations because of its high mechanical strength and high carrier mobility with possible electronic applications.[7,8] For example, it has been recently reported that graphene/$TiO_2$ nanocomposites can render solar cells with a ~15% conversion efficiency.[9] Other applications include the use of graphene as tunable antennas[10] and for the direct generation of terahertz laser pulses on the 100 fs time scale.[11] We note here that terahertz lasing has only been achieved indirectly to date.

In a series of papers, Li et al.[12−16] have reported spectroscopic properties of colloidal graphene quantum dots (GQDs), with solubilizing groups, that were made by a solution chemistry approach. GQDs are 0D quantum-confined systems with potential applications in photovoltaics, and they may also serve as model systems for studying properties of complex carbon materials.[17] The GQDs are held together by well-defined covalent bonds, including the solubilizing groups. Mueller et al. reported on the relaxation pathways in the photoexcited states.[12] From the observation that excitation spectra were highly dependent on the monitored luminescence wavelength, they concluded that relaxation pathways in C132 GQDs vary dramatically within the excited states, resulting in an emitting singlet and triplet state at ~670 and ~750 nm, respectively. Recent reviews of spectroscopic properties of a range of GQDs prepared by a variety of methods have been given in refs 17 and 18. Since a robust understanding of electronic states in GQDs is paramount for taking advantage of their extraordinary electronic properties, we report on our reinvestigation and findings of the spectroscopic properties of C132 GQDs in this article.

## 2. METHODS

**Experiment.** The C132 GQDs were kindly provided by Professor Liang-shi Li of Indiana University and were prepared as described previously by this research group.[15] Absorption spectra of the C132 GQDs in toluene and heptane were recorded on a GBC UV−vis 918 spectrometer in 1 and 5 cm cuvettes. Room temperature and 77 K fluorescence and excitation spectra were measured by using a Jobin Yvon Horiba Spex Fluoromax-3 fluorometer with a liquid nitrogen cryostat built in the laboratory. For temperatures below 77 K a Spex 1704 monochromator equipped with a Hamamatsu R928 photomultiplier was employed. In this latter case the signal was processed by using a Femto DLPCA-200 current voltage amplifier and a Stanford Research Systems SR810 lock-in amplifier. A 10 mW Nd:YAG laser was used as the excitation source, and for excited state lifetime measurements an Oriel model 79111 pulsed nitrogen laser (337 nm) was used. Spectra were fully corrected for the instrumental response. For

Received: March 19, 2014
Revised: June 26, 2014
Published: June 27, 2014

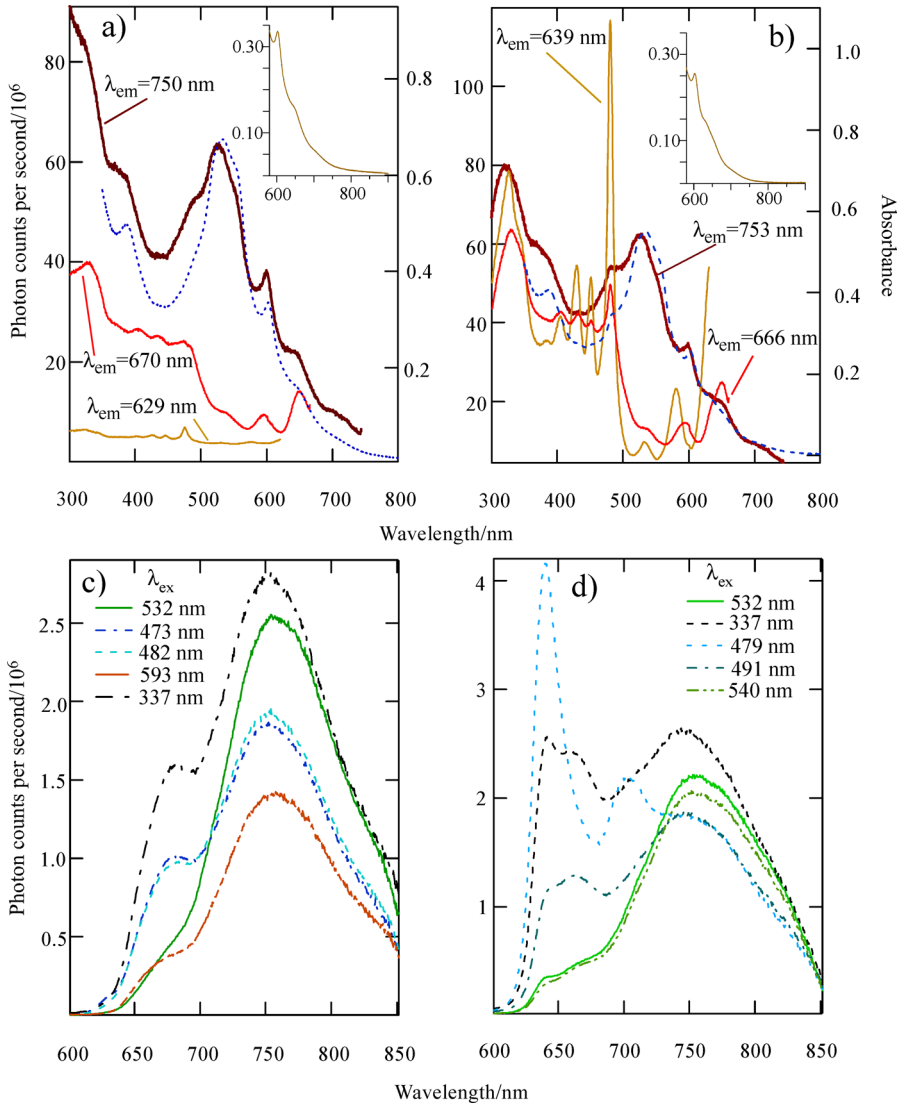


**Figure 1.** Absorption and selective excitation and fluorescence spectra of C132 GQDs at room temperature. (a) Selective excitation spectra as monitored at various emission wavelengths $\lambda_{em}$ together with the absorption spectrum (dashed line) in heptane. The inset shows the absorption spectrum in 600−900 nm region. (b) As in (a) but for toluene. (c) Selectively excited fluorescence spectra for various excitation wavelengths $\lambda_{ex}$ in heptane. (d) As in (c) but for toluene. The absorption spectra were measured in a 5 cm cuvette. All spectra were corrected for the instrumental response.

temperatures below 77 K a Janis/Sumitomo SHI-4.5 closed-cycle refrigerator was employed.

**Theory.** The geometry of the GQDs was first optimized in the $S_0$ electronic ground state based on density-functional theory (DFT). Electronic transitions were calculated in the optimized $S_0$ geometry based on linear response time-dependent density functional theory (TD-DFT), followed by a TD-DFT geometry optimization in the excited electronic $S_1$ state. All these calculations were done with the Gaussian 09 program suite,[19] consistently at the same level of theory with the Becke three-parameter Lee−Yang−Parr hybrid functional (B3LYP) and 6-31G* basis set. This choice of functional and basis set was previously found to give results in good agreement with available experimental data.[20] Visualizations of molecular geometry and orbitals were done with GaussView, version 5.[21] All optimizations were done without any symmetry constraints. We note that the resulting optimized $S_0$ and $S_1$ geometries are not perfectly planar. Absorption spectra were simulated based on the nuclear-ensemble approach.[22] For this purpose the Newton-X program[23] interfaced with Gaussian 09 was used. One-thousand geometries were sampled using a Wigner distribution. The first 20 excitations were calculated for each geometry. For the generation of the simulated spectrum each transition was convoluted with a Gaussian broadening of 0.035 eV. Because of the sampling of different ground state geometries, the spectra calculated within the nuclear ensemble approach are slightly red-shifted compared with the electronic transitions calculated for the optimized ground state geometries. All calculations in this work were done for C132 GQDs dissolved in toluene. The solvent was included based on the polarizable continuum model as implemented in Gaussian 09. Additional side groups on the GQDs were neglected, as those are largely not involved in the lowest optical excitations.

## 3. RESULTS AND DISCUSSION

Figure 1 shows absorption and selective excitation and fluorescence spectra of the C132 GQDs in heptane and toluene. The most pronounced feature in the absorption


dx.doi.org/10.1021/jp502753a | J. Phys. Chem. A 2014, 118, 5189−5195

spectra (dashed lines and insets) is centered around 535 nm in both solvents. On the basis of quantum chemistry calculations (see Methods for details), this feature can be assigned to the bright $S_0 \rightarrow S_3$ and $S_0 \rightarrow S_4$ transitions in the C132 GQDs (cf. Figure 2 and Tables S1 and S2 in the Supporting Information).

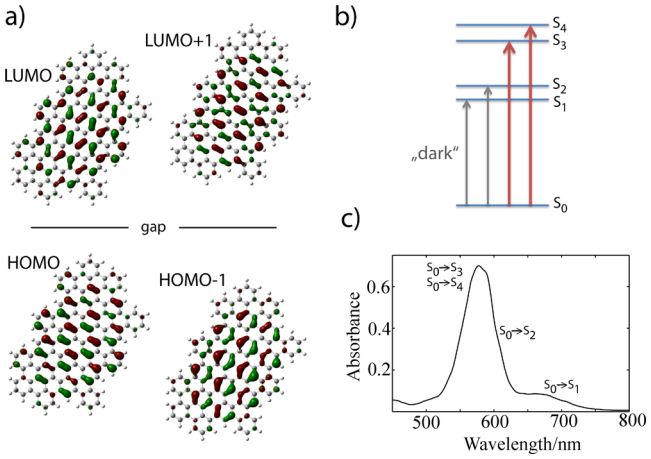


**Figure 2.** (a) Frontier orbitals of the graphene quantum dot that dominate the lowest optical transitions from the electronic ground state $S_0$. (b) Illustration of the four lowest optical transitions. The transitions $S_0 \rightarrow S_1$ and $S_0 \rightarrow S_2$ are optically almost dark with oscillator strengths of only 0.0003 and 0.0756, respectively. (c) Long-wavelength range of simulated absorption spectrum computed using the nuclear-ensemble approach, partly taking into account electron–vibrational coupling.

Figure 2 summarizes the computed results for the C132 GQDs in toluene (see Methods for details of the calculations). The four lowest transitions from the $S_0$ ground state are almost exclusively dominated by the four frontier orbitals shown. The degeneracy of the lowest bright transitions and of the frontier orbitals is lifted because of the absence of symmetry of the C132 GQD. However, we still find that the two lowest singlet excitations $S_0 \rightarrow S_1$ and $S_0 \rightarrow S_2$ are optically almost dark, as was found in a previous calculation[20,24] for higher symmetry GQDs and in other low-dimensional carbon structures, i.e., carbon nanotubes.[25] The oscillator strength we find for the lowest excitation (for the vertical electronic excitation) is about 2 orders of magnitude smaller than the one extracted from the experimental data in Figure 1 (see discussion below). In order to resolve this apparent discrepancy, Figure 2c shows the absorption spectrum obtained using the nuclear-ensemble approach, taking into account coupling of electronic states to the vibrational modes in the quantum dot's ground state. Our calculations only partially include electron–vibrational coupling in the sense that because of the ground-state sampling in the nuclear ensemble approach, spectral contributions for different (nonoptimized) ground state geometries are included in the shown spectra. We note that here we do not analyze the vibrational modes and vibronic progression in the spectra in detail.

Visible is an overall small red-shift of the computed spectrum (peak maximum at 577 nm) compared to the measurements in Figure 1 (peak maximum at 535 nm). However, more importantly, the two low-energy transitions (shoulders) corresponding to the two nominally "dark" electronic transitions are also visible in the calculated spectrum. We note that the absorption feature clearly visible in the experimental spectrum of Figure 1a and Figure 1b at about 600 nm is only visible as a small shoulder on the low-energy side of the main absorption feature in the calculated spectrum due to the finite phenomenological broadening that was employed in the simulation. This result illustrates that because of electron–vibrational coupling, the nominally "dark" low-energy electronic transitions significantly borrow some oscillator strength from the nominally "bright" higher-lying transitions. The main absorption feature in the spectrum in Figure 2c stems from the $S_0 \rightarrow S_3$ and $S_0 \rightarrow S_4$ transitions with oscillator strengths $f = 3.497$ and $f = 1.521$, respectively, for the vertical electronic transitions. To better reproduce the measured spectrum also for wavelengths smaller than 500 nm, electronic transitions higher in energy would have to be included in the calculations. In the present calculations, transitions from $S_0$ into $S_5$ to $S_{20}$ only carry low oscillator strengths. A list of the lowest 20 singlet transitions including oscillator strengths is given in the Supporting Information. For completeness, also a list of the lowest 40 triplet excitations is included in the supplement.

The inset in Figure 1 illustrates that the first absorption band with a noticeable oscillator strength is observed between 700 and 750 nm. From ref 12 it follows that the molar extinction coefficient at around 530 nm is 100 000 $M^{-1}$ $cm^{-1}$, and thus, the extinction coefficient at 720 nm is ~7000 $M^{-1}$ $cm^{-1}$. Assuming a width of this transition of ~1700 $cm^{-1}$ (as estimated from the fluorescence spectra in Figure 1c and Figure 1d, we calculate an oscillator strength of $f \approx 0.03$ using eq 1.

$$f = (4.3 \times 10^{-9}) \int \varepsilon(\bar{\nu})\, d\bar{\nu} \tag{1}$$

From the value of the oscillator strength we estimate an excited state lifetime of ~130 ns, employing eq 2 where $n$ is the refractive index and $g_a$ and $g_b$ are the degeneracy of the excited and ground state, respectively.[26]

$$\tau_{rad} = (1.5 \times 10^{4}) \frac{{\lambda_{ba}}^2}{n[(n^2 + 2)/3]^2} \frac{g_b}{g_a} \frac{1}{f} \tag{2}$$

Room temperature fluorescence spectra of the C132 GQDs in heptane and toluene as excited at various wavelengths are summarized in Figures 1c and 1d.

It is apparent that the main emission band associated with the 530 nm absorption feature is centered at ~750 nm. Two other fluorescence features appear around 630–640 nm and 660–670 nm. The intensity of these features is strongly dependent on the excitation wavelength, and they can be, to some degree, selectively excited. This behavior is strong evidence for different chemical species. We stress here that in fluorescence and excitation spectra minority species may be grossly overemphasized because of variations in quantum efficiency. Hence, impurities at a low percentage levels may still appear as dominant features.

The finding from the selective fluorescence spectra are corroborated by the photoluminescence excitation spectra shown in Figure 1a and Figure 1b as detected at various wavelengths for the C132 GQDs in heptane and toluene. When the emission is detected at 750 nm, the excitation spectrum is a good match of the absorption spectrum; naturally there are some variations due to the partial selectivity in the excitation spectra as the effects of heterogeneity are overcome to some degree. We note here that we have also measured excitation spectra with the wavelength detected around 825 nm where a


dx.doi.org/10.1021/jp502753a | J. Phys. Chem. A 2014, 118, 5189–5195

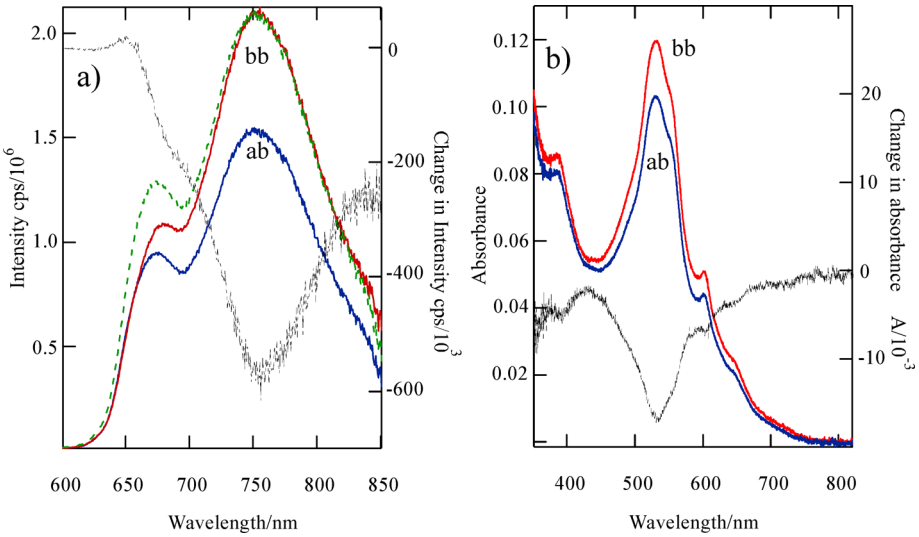


**Figure 3.** Selective bleaching experiment. The (a) fluorescence excited at 337 nm and (b) absorption spectra were measured in heptane before (bb) and after (ab) bleaching in dichloromethane. The dashed line in (a) shows the bleached spectrum renormalized to the 750 nm peak of the unbleached spectrum. The dash–dotted lines in (a) and (b) show the difference spectra (spectrum after bleaching minus spectrum before bleaching).

shoulder is observed in the emission spectra. These spectra are within the experimental accuracy the same as for the 750 nm detection wavelength. In the excitation spectra of the emitters at 629 or 639 nm well pronounced vibrational progressions are observed in the excitation spectra with the vibrational frequency significantly reduced for the higher singlet state at around 480 nm. When the emission is observed at 666 (toluene) or 670 nm (heptane), vibrational progressions are also observed but the transitions appear to be much broader and the electronic origin at around 480 nm carries less intensity. These spectra imply again that the emissions at 629 or 639 and at 670 or 666 nm in toluene and heptane, respectively, are likely due to other species. We note that these transitions appear to be more intense in toluene than in heptane. It appears that there is excitation energy transfer to the 750 nm emitter and that this process is more efficient in heptane than in toluene. In particular, the 639 nm emitter in toluene is much more intense than the 630 nm emitter in heptane. It is possible that there is some molecular association between the impurities (see also the discussion about the heavy atom effect below) and the C132 GQDs and that this association is more pronounced in the case of heptane, in particular for the 639 nm emitter. Possibly, toluene provides some screening effect reducing the energy transfer rate. The idea of energy transfer is corroborated by the observation of a significantly higher intensity of the 639 nm emitter and a reduced 750 nm emission in a 5-fold diluted toluene sample upon excitation at 480 nm (see Supporting Information) because energy transfer can be expected to be strongly concentration dependent. This concentration effect also excludes the explanation of the ∼630 and ∼670 nm emitters being due to H-aggregates. Likewise, J-aggregates, as a possible explanation of the 750 nm emission, can be excluded because this emission is perfectly correlated with the main absorption feature at 530 nm and independent of concentration.

Both the 629 or 639 nm and the 666 or 670 nm emissions carry very little excitation intensity in the 530 nm absorption band; the latter is the main feature of the absorption spectrum. This observation has been interpreted previously by a different branching ratio of the singlet states to the excited states that emit at around 670 and 750 nm.

To provide further evidence that 670 nm (and 630 nm) emission peaks are not due to the main species, C132 GQDs, we conducted photobleaching experiments. The fluorescence was measured in heptane before bleaching. The heptane was then evaporated, and the C132 GQDs were taken up in dichloromethane (dcm). This suspension was then exposed in a 1 cm cuvette to 12 mW of 532 nm light for 3600 s. Subsequently the dcm was evaporated at room temperature, the dry dots were taken up in heptane, and the fluorescence was remeasured. It clearly follows from Figure 3a that the 670 nm emission bleaches at a lower rate than the 750 nm emission; i.e., the bleaching is wavelength selective, indicating strongly that the 670 nm emission is due to an impurity. If the 670 nm emission were intrinsic fluorescence from the C132 GQDs, we would expect that the 532 nm bleaching led to a uniform decrease of the intensity across the emission spectrum.

We note here that the result illustrated in Figure 3a was reproduced several times. As is illustrated in Figure 3b, we have also measured the absorption spectrum before and after bleaching, and it appears that most (absorption) features down to 500 nm are due to the C132 GQDs. However, below 450 nm there is a contribution to the absorption spectrum that bleaches at a slightly lower rate. This is consistent with the observation that excitation wavelengths below 480 nm strongly select the 670 or 666 nm and the 639 or 629 nm emissions for toluene and heptane, respectively. Assuming that the ∼630 and ∼670 nm emissions are due to the C132 GQDs, it would be possible to explain the selective photochemistry by proposing that the photochemical reaction of the C132 GQDs yields a species where the emission of the 670 nm is favored because of a higher population of this state in the relaxation pathway. However, this is an unlikely explanation, since the main features of the absorption and emission spectra remain unchanged.

As previously reported,[12] the 750 nm emission exhibits a very strong external heavy atom effect.[27] We have reinvestigated this effect by adding 1,2-dibromoethane to heptane and toluene solutions. Results are summarized in Table 1, and emission


dx.doi.org/10.1021/jp502753a | J. Phys. Chem. A 2014, 118, 5189−5195

**Table 1. External Heavy Atom Effect by Dibromoethane in the 750 nm Fluorescence of C132 GQDs in Heptane and Toluene[a]**

| toluene | | | heptane | | |
|---|---|---|---|---|---|
| $X$ | $I$(755 nm) | $I_0/I$(755 nm) | $X$ | $I$(755 nm) | $I_0/I$(755 nm) |
| 0.08 | 0.93 | 1.1 | 0.075 | 0.41 | 2.4 |
| 0.17 | 0.8 | 1.3 | 0.145 | 0.16 | 6.3 |
| 0.38 | 0.48 | 2.1 | 0.3 | 0.06 | 17 |
| 0.57 | 0.25 | 4 | 0.55 | 0.03 | 33 |

[a] $X$ denotes the mole fraction. The intensities are normalized to the intensity at $X = 0$, $I_0$.

spectra are shown in the Supporting Information (Figure S1). Upon addition of 1,2-dibromoethane, the shape of the luminescence spectra stays approximately the same with a minor wavelength shift due to the change in the dielectric constant of the solvent mixture.

Interestingly, the heptane suspension is subject to a significantly stronger heavy atom effect than the toluene suspension as a function of the mole fraction of 1,2-dibromoethane. Stern–Volmer plots of $I_0/I$ against the quencher concentration reveal a sizable superlinearity; this is possibly due to a contribution by static quenching caused by the molecular association of the 1,2-dibromoethane with the C132 GQDs. We note here that the quencher concentration is very high and perfect linearity in a Stern–Volmer plot cannot be expected. The significantly higher quenching effect may be due to the lower viscosity of heptane in comparison with toluene and/or a higher molecular association of the quencher with the GQDs. It is also possible that the singlet–triplet spacing varies between heptane and toluene because of the dielectric constant, resulting in a larger heavy atom effect for heptane. Importantly, we cannot exclude that the toluene shields the GQDs, dynamically or statically, to a certain extent. This latter explanation is consistent with the observation that the ~630 and ~670 nm species appear to be subject to

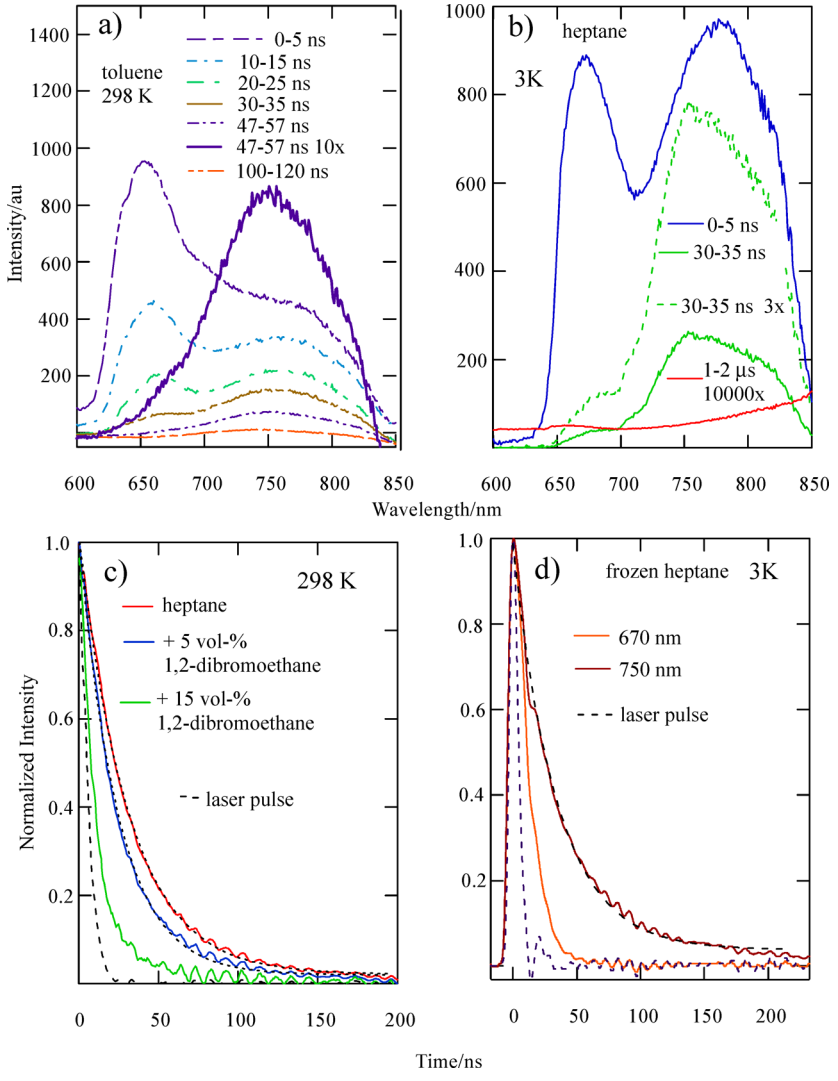


**Figure 4.** Time-resolved (TR) fluorescence spectra and excited state lifetime measurements of the graphene quantum dots with pulsed 337 nm $N_2$ laser excitation. (a) and (b) show TR spectra in toluene at 298 K and frozen heptane at 3 K, respectively. The time gate at which the emission was observed and magnification multipliers are indicated. (c) shows lifetime measurements of the graphene quantum dots for a heptane suspension and for heptane suspensions to which 5 and 15 vol % 1,2-dibromoethane were added. In (d) the decay is shown for the 750 and 670 nm emission in frozen heptane at 3 K. The dashed line in (c) and (d) shows the $N_2$ laser pulse.


dx.doi.org/10.1021/jp502753a | J. Phys. Chem. A 2014, 118, 5189–5195

significantly faster excited-state energy transfer to the C132 GQDs in heptane compared to toluene (see above).

The observed heavy atom effect indicates that the C132 GQDs must have a triplet state not far below the 750 nm emitting state, consistent with the decreased singlet−triplet energy spacing due to the large conjugation size and the reduced exchange interaction.[20] In agreement with this statement we note that the DFT calculations (see Supporting Information) predict a $S_1-T_1$ splitting of ∼3300 $cm^{-1}$ in toluene.

The heavy atom effect is again in contradiction with the initial assignment of the 670 and 750 nm emissions to intrinsic $S_1 \rightarrow S_0$ and $T_1 \rightarrow S_0$ transitions by Mueller et al.[12] The (external) heavy atom effect strongly enhances the internal system conversion (ISC) $S_1 \rightarrow T_1$; i.e., quenching of the $S_1$ state and an increase in $T_1 \rightarrow S_0$ intensity are usually observed.[27] Hence, with the energy level assignment given in ref 12 a massive drop of the 670 nm emission with an increase of the 750 nm emission would be expected; however, this is not the case and the heavy atom effect quenches the 750 nm emission to a much greater extent than the 670 (630, 640) nm emissions. This indicates again that the 670 (630, 640) nm transitions are not the $S_1$ state of the C132 GQDs but indeed due to other species. The quenching of the 750 nm emission is consistent with it being due to the $S_1 \rightarrow S_0$ transition, and the quenching is based on the ISC $S_1 \rightarrow T_1$. If the 750 nm emission would be the (lowest-excited) $T_1$ state, in addition to a massive increase in its population, the radiative deactivation rate to the $S_0$ ground state would be increased and the 750 nm emission would be strongly enhanced by the ISC. The opposite is observed.

Figure 4 shows measurements of time-resolved emission spectra (TRS) and excited state lifetimes, respectively, upon excitation of the GQDs at 337 nm with a pulsed $N_2$ laser. The TRS displayed in Figure 4 a and Figure 4b confirm that the 750 nm emission decays on the 30 ns time scale, in contrast to the ∼630 and ∼670 nm emissions that decay on the 10 ns time scale. From these spectra and lifetime measurements it follows that there may be a minor component at 825 nm that displays a longer lifetime (approximately 200 ns). This is possibly due to the triplet state.

At room temperature, the lifetime of the 750 nm photoluminescence is 31 ns in heptane. In comparison a slight increase of the lifetime to 34 ns is observed in frozen heptane at 3 K. In comparison, the 670 nm emitter (impurity) has a significantly shorter lifetime. The measured lifetimes are summarized in Table 2.

**Table 2. Summary of Measured Excited State Lifetimes at Room Temperature**

| solvent | emission wavelength, nm | lifetime, ns |
|---|---|---|
| toluene | 640 | 10 ± 3 |
| toluene | 743 | 26 ± 2 |
| heptane | 670 | 8 ± 3 |
| heptane | 750 | 31 ± 2 |

From the lifetime and the calculated oscillator strength we estimate a relatively high quantum efficiency of ∼0.2 for the 750 nm emission.

The relatively long excited state lifetime of the graphene quantum dots is consistent with the oscillator strength observed in the absorption spectrum. The quantum chemical calculations as discussed above clearly confirm that the lowest excited singlet states are "near-dark states", i.e., singlet states with very low oscillator strengths.

The electronic oscillator strength we computed for $S_1$ in emission ($f$ = 0.0003) is the same as in absorption and much lower than found in the measurements. However, also in emission, borrowing of oscillator strength from higher-lying transitions through electron-vibrational coupling is likely to occur in the real system. This mechanism was demonstrated to have a pronounced effect on our simulated absorption spectrum in Figure 2c.

In our measurements, we have been unable to observe a transient on the microsecond time scale between 750 and 800 nm as has been reported previously. We conclude that this reported observation may have been due to the phosphorescence of an impurity.

The remaining question is the origin of the ∼630 and 670 nm emissions; above we have been able to rule out J- and H-aggregates. It is possible that these emitters are C132 GQDs with some structural defects or different symmetry. However, it would be surprising that minor structural or symmetry changes would lead to vastly different behavior, in particular to spectra that are somewhat reminiscent of polycyclic hydrocarbons with well-defined vibrational progressions. More likely explanations for these emitters include fragments of the C132 GQDS; it is also possible that these species are oxidized GQDs. However, for the latter we would expect similar broad spectroscopic features as for the main C132 GQDs.[12,13] Further work would be needed to identify the chemical properties of these impurities; however, we note here again that impurities at very low concentration can have a significant impact on photoluminescence and excitation.

## 4. CONCLUSIONS

A range of spectroscopic experiments, including selective fluorescence and excitation spectra, time-resolved spectra, external heavy atom experiments, and wavelength selective bleaching experiments, were undertaken on C132 GQDs at room and low temperatures. In particular, the wavelength selective photobleaching yields strong evidence for the identification of the intrinsic emission of the C132 GQDs at 750 nm and shows that it is safe to assign emitters at around 670 and 640 nm to chemically different species. The spectra of these impurities appear to be quite intense in the fluorescence and excitation spectra because of their higher quantum efficiency and narrower features with well-defined vibrational progressions. Thus, it is possible to identify the intrinsic features of the C132 GQDs: the main absorption and emission feature are centered around 530 and 750 nm, respectively, and the two transitions have a very similar overall line shape. From a comparison of the absorption spectrum and the emission spectrum it follows that the $S_0 \rightarrow S_1$ electronic origin is around 720−730 nm and the main intensity component must be of vibrational nature in agreement with quantum chemical nuclear ensemble calculations. The relatively long lifetime of 30 ns and the relatively low oscillator strength of the transition are in qualitative accord with the quantum chemical calculations that indicate near-dark low-lying singlet states. Furthermore, the singlet state at 750 nm gets quenched upon the addition of heavy atom solvents in agreement with expectations.


dx.doi.org/10.1021/jp502753a | J. Phys. Chem. A 2014, 118, 5189−5195

## ■ ASSOCIATED CONTENT

### Supporting Information

Full author list for refs 8 9, and19, vertical excitation energies for the first 20 singlet states, vertical excitation energies for the first 40 triplet states, spectra showing the observed heavy atom effect, and photoluminescence spectrum for diluted sample. This material is available free of charge via the Internet at http://pubs.acs.org.

## ■ AUTHOR INFORMATION


### Corresponding Author

*E-mail: h.riesen@adfa.edu.au.


### Author Contributions

The manuscript was written through contributions of all authors. All authors have given approval to the final version of the manuscript.

### Notes

The authors declare no competing financial interest.

## ■ ACKNOWLEDGMENTS

We thank Professor Liang-shi Li, Indiana University, Bloomington, IN, for providing us with graphene quantum dots. The Paderborn group acknowledges financial support from the DFG (Grant GRK 1464) and a grant for computing time at PC$^2$ Paderborn Center for Parallel Computing. C.W. is grateful for his Ph.D. scholarship from the Friedrich-Ebert-Stiftung.

## ■ REFERENCES


(1) Kroto, H. W.; Heath, J. R.; O'Brien, S. C.; Curl, R. F.; Smalley, R. E. C-60 Buckminsterfullerene. *Nature* **1985**, *318*, 162−163.

(2) Boehm, H. P. The First Observation of Carbon Nanotubes. *Carbon* **1997**, *35*, 581−584.

(3) Geim, A. K. Graphene: Status and Prospects. *Science* **2009**, *324*, 1530−1534.

(4) Güçlü, A. D.; Potasz, P.; Hawrylak, P. Excitonic Absorption in Gate-Controlled Graphene Quantum Dots. *Phys. Rev. B* **2010**, *82*, 155445.

(5) Mochalin, V. N.; Shenderova, O.; Ho, D.; Gogotsi, Y. The Properties and Applications of Nanodiamonds. *Nat. Nanotechnol.* **2012**, *7*, 11−23.

(6) Doherty, M. W.; Manson, N. B.; Delaney, P.; Jelezko, F.; Wrachtrup, J.; Hollenberg, L. C. L. The Nitrogen-Vacancy Colour Centre in Diamond. *Phys. Rep.* **2013**, *528*, 1−45.

(7) Geim, A. K.; Novoselov, K. S. The Rise of Graphene. *Nat. Mater.* **2007**, 183−191.

(8) Novoselov, K. S.; Morozov, S. V.; Mohinddin, T. M. G.; Ponomarenko, L. A.; Elias, D. C.; Yang, R.; Barbolina, I. I.; Blake, P.; Booth, T. J.; Jiang, D.; et al. Electronic Properties of Graphene. *Phys. Status Solidi B* **2007**, *244*, 4106−4111.

(9) Wang, J. T.-W.; Ball, J. M.; Barea, E. M.; Abate, A.; Alexander-Webber, J. A.; Huang, J.; Saliba, M.; Mora-Sero, I.; Bisquert, J.; Snaith, H. J.; et al. Low-Temperature Processed Electron Collection Layers of Graphene/$TiO_2$Nanocomposites in Thin Film Perovskite Solar Cells. *Nano Lett.* **2014**, *14*, 724−730.

(10) Filter, R.; Farhat, M.; Steglich, M.; Alaee, R.; Rockstuhl, C.; Lederer, F. Tunable Graphene Antennas for Selective Enhancement of THz-Emission. *Opt. Express* **2013**, *21*, 3737−3745.

(11) Gierz, I.; Petersen, J. C.; Mitrano, M.; Cacho, C.; Turcu, I. C. E.; Springate, E.; Stohr, A.; Kohler, A.; Starke, U.; Cavalleri, A. Snapshots of Non-Equilibrium Dirac Carrier Distributions in Graphene. *Nat. Mater.* **2013**, *12*, 1119−1124.

(12) Mueller, M. L.; Yan, X.; McGuire, J. A.; Li, L. S. Triplet States and Electronic Relaxation in Photoexcited Graphene Quantum Dots. *Nano Lett.* **2010**, *10*, 2679−2682.

(13) Li, L. S.; Yan, X. Colloidal Graphene Quantum Dots. *J. Phys. Chem. Lett.* **2010**, 2572−2576.

(14) Yan, X.; Cui, X.; Li, B. S.; Li, L. S. Large, Solution-Processable Graphene Quantum Dots as Light Absorbers for Photovoltaics. *Nano Lett.* **2010**, *10*, 1869−1873.

(15) Yan, X.; Cui, X.; Li, L. S. Synthesis of Large, Stable Colloidal Graphene Quantum Dots with Tunable Size. *J. Am. Chem. Soc.* **2010**, *132*, 5944−5945.

(16) Yan, X.; Li, L. S. Solution-Chemistry Approach to Graphene Nanostructures. *J. Mater. Chem.* **2011**, *21*, 3295−3300.

(17) Zhang, Z. P.; Zhang, J.; Chen, N.; Qu, L. T. Graphene Quantum Dots: An Emerging Material for Energy-Related Applications and Beyond. *Energy Environ. Sci.* **2012**, *5*, 8869−8890.

(18) Li, L.; Wu, G.; Yang, G.; Peng, J.; Zhao, J.; Zhu, J.-J. Focusing on Luminescent Graphene Quantum Dots: Current Status and Future Perspectives. *Nanoscale* **2013**, *5*, 4015−4039.

(19) Frisch, M. J.; Trucks, G. W.; Schlegel, H. B.; Scuseria, G. E.; Robb, M. A.; Cheeseman, J. R.; Scalmani, G.; Barone, V.; Mennucci, B.; Petersson, G. A.; et al. *Gaussian 09*, revision B.01; Gaussian, Inc.: Wallingford, CT, 2009.

(20) Schumacher, S. Photophysics of Graphene Quantum Dots: Insights from Electronic Structure Calculations. *Phys. Rev. B* **2011**, *83*, 081417.

(21) Dennington, R.; Keith, T.; Millam, J. *GaussView*, version 5; Semichem Inc.: Shawnee Mission, KS, 2009.

(22) Crespo-Otero, R.; Barbatti, M. Spectrum Simulation and Decomposition with Nuclear Ensemble: Formal Derivation and Application to Benzene, Furan and 2-Phenylfuran. *Theor. Chem. Acc.* **2012**, *131*, 1237.

(23) Barbatti, M.; Granucci, G.; Persico, M.; Ruckenbauer, M.; Vazdar, M.; Eckert-Maksic, M.; Lischka, H. The On-the-Fly Surface-Hopping Program System NEWTON-X: Application to ab Initio Simulation of the Nonadiabatic Photodynamics of Benchmark Systems. *J. Photochem. Photobiol., A* **2007**, *190*, 228−240.

(24) Ozfidan, I.; Korkusinski, M.; Güçlü, A. D.; McGuire, J. A.; Hawrylak, P. Microscopic Theory of Optical Properties of Colloidal Graphene Quantum Dots. *Phys. Rev. B* **2014**, *89*, 085310.

(25) Kilina, S.; Tretiak, S.; Doorn, S. K.; Luo, Z.; Papadimitrakopoulos, F.; Piryatinski, A.; Saxena, A.; Bishop, A. R. Cross-Polarized Excitons in Carbon Nanotubes. *Proc. Natl. Acad. Sci. U.S.A.* **2008**, *105*, 6797−6802.

(26) Solomon, E. I., Lever, A. B. P., Eds. *Inorganic Electronic Structure and Spectroscopy*; Wiley-Interscience: Hoboken, NJ, 2006; Vol. *I*.

(27) McGlynn, S. P.; Azumi, T.; Kinoshita, M. *Molecular Spectroscopy of the Triplet State*; Prentice-Hall: Englewood Cliffs, NJ, 1969; p xiii, 434 pp.


## ■ NOTE ADDED AFTER ASAP PUBLICATION

This article posted ASAP on July 8, 2014. The reference numbers in the following locations have been revised: Methods section, paragraph 2; Results and Discussion section, paragraph 2, sentence 4, and paragraph 12, sentence 2. The correct version posted July 17, 2014.